BIOCHEMISTRY
including biophysical chemistry & molecular biology

Article

pubs.acs.org/biochemistry

Ascorbic Acid Reduction of Compound I of Mammalian Catalases Proceeds via Specific Binding to the NADPH Binding Pocket

Hans-Gert Korth,*[,†] Ann-Cathérine Meier,[‡] Oliver Auferkamp,[‡] Willi Sicking,[†] Herbert de Groot,[‡] Reiner Sustmann,[†] and Michael Kirsch*[,‡]

[†]Institut für Organische Chemie, Universität Duisburg-Essen, 45117 Essen, Germany

[‡]Institut für Physiologische Chemie, Universitätsklinikum Essen, 45122 Essen, Germany

Supporting Information

ABSTRACT: Mammalian (Clade 3) catalases utilize NADPH as a protective cofactor to prevent one-electron reduction of the central reactive intermediate Compound I (Cpd I) to the catalytically inactive Compound II (Cpd II) species by re-reduction of Cpd I to the enzyme's resting state (ferricatalase). It has long been known that ascorbate/ascorbic acid is capable of reducing Cpd I of NADPH-binding catalases to Cpd II, but the mode of this one-electron reduction had hitherto not been explored. We here demonstrate that ascorbate-mediated reduction of Cpd I, generated by addition of peroxoacetic acid to NADPH-free bovine liver catalase (BLC), requires specific binding of the ascorbate anion to the NADPH binding pocket. Ascorbate-mediated Cpd II formation was found to be suppressed by added NADPH in a concentration-dependent manner, for the achievement of complete suppression at a stoichiometric 1:1 NADPH:heme concentration ratio. Cpd I → Cpd II reduction by ascorbate was similarly inhibited by addition of NADH, $NADP^+$, thio-$NADP^+$, or NAD^+, though with 0.5-, 0.1-, 0.1-, and 0.01-fold reduced efficiencies, respectively, in agreement with the relative binding affinities of these dinucleotides. Unexpected was the observation that although Cpd II formation is not observed in the presence of $NADP^+$, the decay of Cpd I is slightly accelerated by ascorbate rather than retarded, leading to direct regeneration of ferricatalase. The experimental findings are supported by molecular mechanics docking computations, which show a similar binding of NADPH, $NADP^+$, and NADH, but not NAD^+, as found in the X-ray structure of NADPH-loaded human erythrocyte catalase. The computations suggest that two ascorbate molecules may occupy the empty NADPH pocket, preferably binding to the adenine binding site. The biological relevance of these findings is discussed.

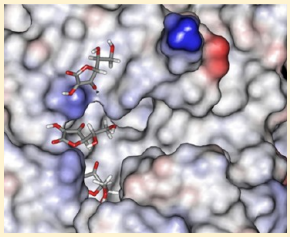

Catalases are ubiquitous and long-known enzymes that in almost all aerobically respiring organisms regulate and detoxify endogenously formed hydrogen peroxide by disproportionation to water and molecular oxygen.[1−10] Mammalian catalases are monofunctional (Class 1), tetrameric heme catalases and are further classified as Clade 3 [small subunit (<60 kDa), His III, heme b] catalases. A unique feature of essentially all Clade 3 catalases, not found in Clade 1 and 2 catalases, is the additional binding of NADPH/$NADP^+$ as a cofactor.[11] X-ray data show that the NADPH/$NADP^+$ ligand is bound in a pocket at the surface of each subunit, at a shortest distance of ∼13 Å from the heme group.[12−16] The current view is that the bound NADPH represents a protective factor for the enzyme, acting by reducing the key reactive intermediate, Compound I (Cpd I; $por^{\bullet+}Fe^{IV}{=}O$), back to the enzyme's resting state, ferricatalase ($porFe^{III}$), in case of H_2O_2 fluxes that are too low to maintain the normal catalytic cycle (Scheme 1).[2,7,9,11,16−24] By this method, the self-oxidation of the enzyme and/or the reduction by external one-electron donors to give the catalytically inactive species Compound II (Cpd II) is prevented. In Cpd II, the porphyrin radical cation of Cpd I has been reduced back to the intact porphyrin. Recent studies showed that Cpd II preferably exists in its protonated form, $porFe^{IV}{-}OH^+$, rather than as $porFe^{IV}{=}O$.[25,26]

Scheme 1. Simplified Catalytic Cycle of Clade 3 Catalases

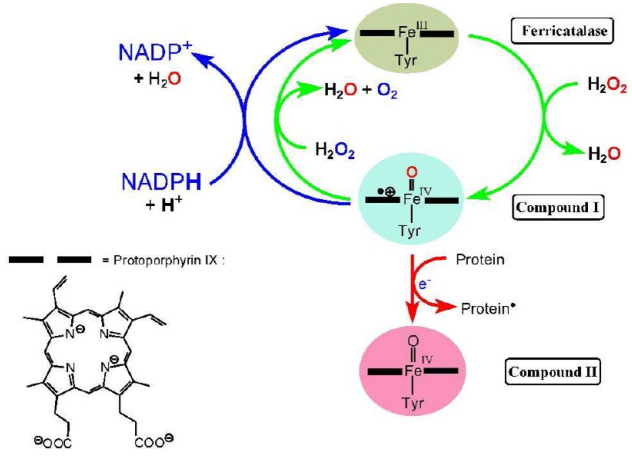

In 2005, a study revealed that the $NADP^+$ formed during the regeneration of ferricatalase by bound NADPH remains bound to the enzyme pocket and that the protective functionality of

Received: November 29, 2011
Revised: May 21, 2012
Published: May 22, 2012

NADPH is preserved by re-reduction of the bound $NADP^+$ by external (unbound) NADPH rather than by NADPH−$NADP^+$ exchange.[27] It should also be noted that NADH and NAD^+ bind to the enzyme pocket, with the strength of binding (matching the efficiency of Cpd II suppression) decreasing in the following order: NADPH > NADH ≫ $NADP^+$ > NAD^+.[1,2,11,27,28]

In a recent review, Kirkman and Gaetani called mammalian catalase "a venerable enzyme with new mysteries".[9] A major mystery addressed in their review is the detailed mechanism by which NADPH reduces Cpd I back to ferricatalase. Because of the kinetic peculiarities of this process, it has been proposed that an additional high-valent heme iron intermediate should be involved that must be in equilibrium with Cpd I.[2,9,24] On the basis of the analysis of the available X-ray structures of catalases and quantum-chemical density functional theory (DFT) calculations, we recently proposed a mechanism for the NADPH path of the catalytic cycle.[29] The X-ray data disclosed a highly conserved molecular arrangement in the heme−NADPH region and, with one exception (see ref 56 in ref 29), a conserved water molecule as a nearest neighbor of the 4-vinyl group of the heme. The calculations suggested that this water molecule plays a pivotal role in the reduction process. Upon formation of Cpd I, i.e., oxidation of the heme porphyrin to its radical cation, a reversible nucleophilic addition of a hydroxyl anion released from this water molecule to the 4-vinyl group of the heme becomes energetically and kinetically feasible. Thereby, an adduct, HO−por$^{\bullet}$$Fe^{IV}$=O, is formed, which could be the proposed additional heme iron intermediate. Simultaneous proton shifts toward the NADPH binding site then facilitate the flow of electrons from NADPH to this heme species. On two-electron reduction of HO−por$^{\bullet}$$Fe^{IV}$=O, the addition of OH^- is instantaneously reversed to give directly ferricatalase, thereby preventing Cpd II formation (see Scheme 2 of ref 29). It should be emphasized that this mechanism is in accord with all published experimental observations.

There are a few low-molecular weight compounds other than H_2O_2 that are known to react with Cpd I of catalase. Ascorbic acid/ascorbate ($AscH_2$/$AscH^-$) is a prominent example of such an "electron/hydrogen donor". In 1947, Chance noted the acceleration of decomposition of Cpd I by ascorbic acid,[30] and Lemberg and Foulkes observed a change in the UV−vis spectrum of catalase upon its interaction with ascorbic acid.[31] The new spectroscopic features were identified by Chance as Cpd II,[32−35] the one-electron reduction product of Cpd I. (Catalase Cpd II was first spectroscopically detected by Stern in 1936.[36,37]) According to the classification of electron/hydrogen donors for catalases introduced by Keilin and Nicholls,[38] ascorbic acid is a "D1 group" donor, i.e., a one-electron donor that converts Cpd I only to Cpd II. Hexacyanoferrate(II) is another member of this group. Although one-electron reduction of Cpd I (which corresponds to catalase/H_2O_2 mixtures) by ascorbate has several times been mentioned in the literature, there seems to be no study specifically devoted to the structural and mechanistic details of this reaction. Recently, it has been reported that ascorbic acid quenches the tryptophan fluorescence of bovine liver catalase (BLC) in a concentration-dependent manner. Li et al.[39] concluded that the quenching process requires specific binding of ascorbic acid to the enzyme, but the mode of interaction was not further elaborated or discussed. It is noteworthy that in our computational study mentioned above we found that upon one-electron reduction of HO−por$^{\bullet}$$Fe^{IV}$=O, the proposed addition of OH^- is readily reversed, directly resulting in the formation of Cpd II.[29] We thus suspected that the ascorbate-mediated reduction of Cpd I of NADPH-binding catalases would occur only via (competitive) binding of ascorbate to the NADPH pocket. We here demonstrate that this is indeed true. It was found that substantial reduction of Cpd I to Cpd II takes place only in the absence of NADPH, $NADP^+$, NADH, or, to a much lower extent, NAD^+, proving that docking of ascorbic acid/ascorbate is blocked by these dinucleotides. This finding is supported by molecular mechanics (MM) docking computations.

MATERIALS AND METHODS

Catalase from bovine liver (BLC, suspension form, EC 1.11.1.6), glucose oxidase from *Aspergillus niger* (lyophilized, EC 1.1.3.4), glucose 6-phosphate (disodium salt), xanthine oxidase from bovine cow milk (lyophilized, EC 1.1.3.22), NADPH, and NADH were purchased from Roche Biochemicals (Mannheim, Germany). Merck (Darmstadt, Germany) was the source of L-(+)-ascorbic acid. Diethylenetriaminepentaacetic acid (DTPA), xanthine, glucose, K_2HPO_4, KH_2PO_4, Chelex-100 (chelating resin, iminodiacetic acid), and dialysis tubes were obtained from Sigma Chemicals (Deisenhofen, Germany). The peroxoacetic acid solution was a product of Fluka (Deisenhofen, Germany), and ethanol was purchased from Riedel de Haën (Deisenhofen, Germany).

All solutions were prepared with highly purified water received from TKA-LAB (Niederelbert, Germany).

In general, phosphate buffer solutions (50 mM, pH 7.4) were exposed for >12 h to the chelating resin Chelex-100 (1.5 g/50 mL) as described previously.[40] Afterward, DTPA (100 μM) was added. The xanthine stock solution was prepared with an alkaline K_3PO_4 (50 mM) solution, which was treated with Chelex-100 as described above.

Stock solutions of reagents were freshly prepared on a daily basis and were stored on ice for the duration of the experiments.

The stock solution of catalase was mixed (1:5 v/v) with a phosphate buffer solution (50 mM, pH 7.4) and was then incubated for ∼4 min at 37 °C until the solutions became clear and their color had changed to green. Then, the enzyme solution (∼5 mL) was dialyzed against a phosphate buffer solution (5 L, 50 mM, pH 7.4, 4 °C) for 1 day, including two exchanges of the dialysis solution.

All reactions were performed in phosphate buffer (50 mM, 100 μM DTPA, pH 7.4) at 25 °C. Steady-state flows of H_2O_2 were generated enzymatically with a glucose oxidase system in glucose (10 mM)-enriched buffer. In the hydrogen peroxide and superoxide radical production experiments, a xanthine (100 μM)/xanthine oxidase system in phosphate buffer in the absence of superoxide dismutase was employed.

To keep the enzyme in the resting Fe(III) state, i.e., for reducing unintentionally produced Cpd I and Cpd II, a heme equivalent amount of ethanol was added prior to the start of the experiments.

Electronic absorption spectra were monitored with a Specord S100 diode array spectrometer from Analytic Jena (Jena, Germany), using a micro quartz cuvette in a thermostated bath (25 °C).

For the determination of ferricatalase, Cpd II, and Cpd I, molar absorptivities of 3.24×10^5 (ε_{405}),[41] 3.2×10^4 (ε_{435}),[42] and 5.7×10^3 M^{-1} cm^{-1} (ε_{660}),[43] respectively, were used.

For the preparation of high concentrations of Cpd I, peroxoacetic acid is a suitable reagent.[44] To remove undesired

dx.doi.org/10.1021/bi2017602 | *Biochemistry* 2012, 51, 4693−4703

hydrogen peroxide contamination, the peroxoacetic acid stock solution was incubated for ~30 min with 8 nM catalase at room temperature.[44] The thus purified stock solution was stored on ice until it was used. For Cpd I formation, ferricatalase was treated with 3 equiv of peroxoacetic acid; the highest Cpd I concentration was reached after an incubation period of ~15 s at 25 °C.

Data analysis was performed with SigmaPlot version 10 (Systat Software, Inc.). Data points and error bars given in the figures refer to averages of three or four independent measurements.

Molecular mechanics (MM) docking studies were performed with MacroModel 9.8 (Schrödinger, LLC, New York) employing the OPLS_2005 force field. The aqueous environment was modeled by the dielectric continuum model. As a starting structure for the docking calculations, the experimental X-ray structure of HEC with bound $NADP^+$ [Protein Data Bank (PDB) entry 1DGF, subunit A] was used. Hydrogen atoms were added by using standard bond lengths and angles. Bound water molecules were omitted from the calculations. For NADPH docking, the nicotinamide group was converted to a dihydronicotinamide unit without significantly altering the positions of the heavy atoms. For ascorbate docking, the lowest-energy CBS-QB3-calculated structure of $AscH^-$ (see Figure S6 of the Supporting Information) was taken as the starting structure. One to four ascorbate molecules were placed at random in the pocket. In all docking runs, the protein structure was kept frozen, but the structure of the ligands was always fully optimized. Quantum-chemical density functional theory (DFT) computations were conducted with the Gaussian 09 suite of programs.[45] Molecular graphics were created with Discovery Studio Visualizer version 2.5 (Accelrys Software Inc., San Diego, CA).

RESULTS

Inhibition of Ascorbate-Induced Formation of Cpd II by NADPH. Upon addition of a 3-fold excess (30 μM) of peroxoacetic acid to NADPH-free bovine liver catalase (BLC) (2.5 μM, corrresponding to 10 μM heme centers), the characteristic UV–vis absorption of Cpd I at 660 nm (λ_{max}) (Figure 1a; for comparison, spectra from the literature are reproduced in Figure S1 of the Supporting Information) built up within 10 s, in agreement with the rate constants for Clade 3 catalases given in previous reports.[3,44,46,47] In the absence of any additives, the 660 nm absorption decayed in an apparent sigmoid fashion (Figure 1b; see also Figure 3b) with a half-life of ~300 s (time-dependent spectra in the 500–800 nm range are shown in Figure S2 of the Supporting Information). Similar time dependencies, which reflect the reduction of Cpd I by an "endogenous donor" from the protein, have been reported previously.[43,48−50]

When NADPH (1 mM) was added 60 s after the first spectrum had been recorded, the Cpd I absorption decayed ~10 times faster, in an apparent first-order process with a rate constant k_1 of $(1.8 \pm 0.1) \times 10^{-2}$ s^{-1} at 25 °C, corresponding to a half-life of ~38 s, again in good agreement with previous observations.[43]

As expected,[30] addition of ascorbic acid (1 mM) also accelerated the decay of Cpd I ($t_{1/2}$ ~ 120 s), though ascorbic acid was less effective than NADPH. The decay clearly followed a sigmoid time dependence, which reasonably can be assumed to be caused by regeneration of Cpd I by excess peroxoacetic acid in the early stages of the reaction, which was supported by kinetic simulations (data not shown).

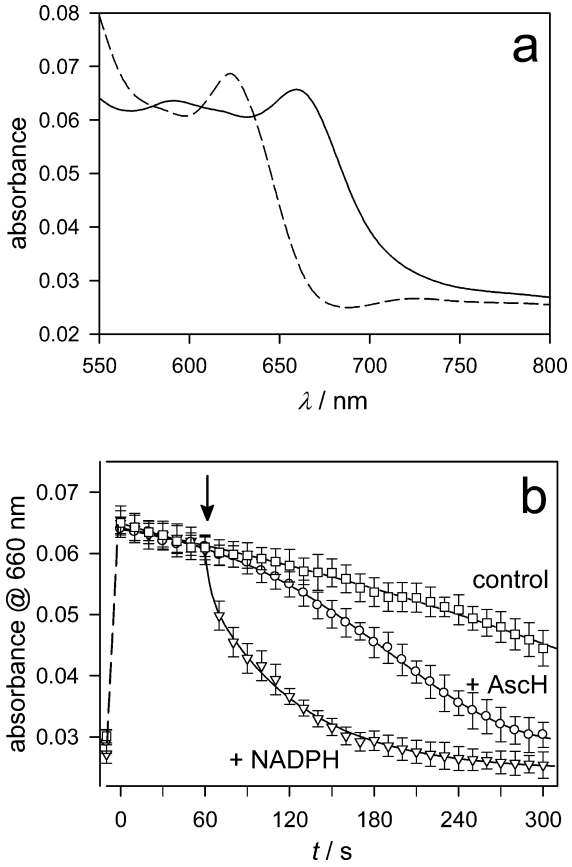

Figure 1. (a) Visible spectrum of Cpd I (—), recorded 10 s after NADPH-free BLC (2.5 μM) (– – –) had been mixed with peroxoacetic acid (30 μM) in phosphate buffer (pH 7.4) at 25 °C. (b) Time dependence of the absorption of Cpd I at 660 nm (λ_{max}), in the absence of any additives (□), in the presence of 1 mM NADPH (▽), and in the presence of 1 mM ascorbic acid (○). The arrow marks the point of addition of NADPH or ascorbic acid. Solid lines show empirical least-squares fits to sigmoidal (□ and ○) and exponential (▽) functions. Data points before time zero show background absorption prior to addition of peroxoacetic acid.

The formation of Cpd II was monitored at 435 nm, the isosbestic point between ferricatalase and Cpd I.[5] In accord with previous work,[5,33,38,51,52] in the absence of additional reductants, the buildup of the Cpd II absorption followed an apparent first-order rate law to approach a constant, rather low level within ~90 s (data not shown). This suggested that under the given conditions the concentration of Cpd II reached a steady-state level corresponding to ~30% of the total heme centers due to subsequent reduction to ferricatalase (see below). Similar time dependencies for Cpd II of BLC have been reported previously.[43,50] In marked contrast, addition of excess ascorbate (300 μM) after 60 s caused a strong, exponential buildup of the absorption of Cpd II (Figure 2a), with a half-life of ~32 s [$k_{1app} = (2.2 \pm 0.2) \times 10^{-2}$ s^{-1}].[a] The ascorbate-induced formation of Cpd II was effectively suppressed by simultaneous addition of increasing amounts (2–75 μM) of NADPH. Even at 2.0 μM NADPH, the formation of Cpd II was significantly (~50%) reduced, and it was completely suppressed at ≥25 μM. The kinetic traces of Figure 2 further reveal a continuous degradation of the initially produced Cpd II at higher NADPH concentrations, in agreement with the

dx.doi.org/10.1021/bi2017602 | Biochemistry 2012, 51, 4693–4703

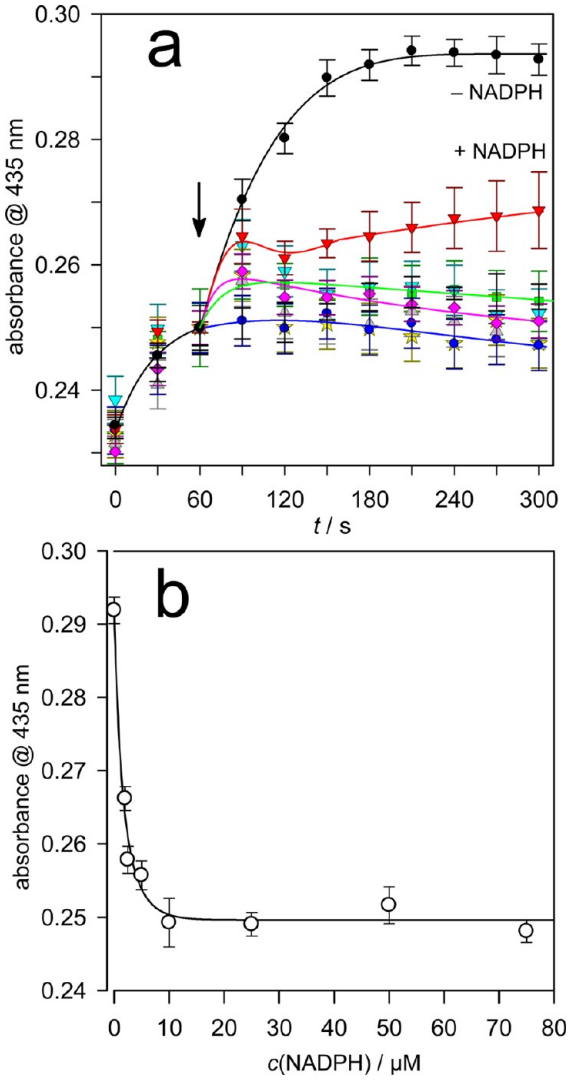

Figure 2. (a) Effect of NADPH on the formation of Cpd II from reaction of NADPH-free BLC (2.5 μM) with peroxoacetic acid (30 μM) in phosphate buffer (pH 7.4) at 25 °C, monitored at 435 nm (λ_{max}). Sixty seconds after the reactants had been mixed, only ascorbic acid (300 μM) (●) or, simultaneously, ascorbic acid (300 μM) and increasing amounts of NADPH were added (arrow). The final concentrations of NADPH were 2.0 (red triangles), 2.5 μM (green squares), 5.0 μM (magenta diamonds), 10.0 μM (cyan triangles), 25.0 μM (yellow stars), 50.0 μM (gray triangles), and 75 μM (blue circles). The solid lines (empirical fits for data at 2.0, 2.5, 5.0, and 75 μM NADPH) are just intended to guide the eye. (b) Dependence of the UV–vis absorption intensity of Cpd II 120 s after the addition of ascorbate on the concentration of NADPH (data from panel a). The solid line is a single-exponential fit.

"reverse" hypothesis of action of NADPH; that is, NADPH not only prevents formation of Cpd II but also is capable of reducing it, albeit slowly, back to ferricatalase.[17,24,28]

The plot of the absorbances of Cpd II 120 s after addition of $AscH^-$, i.e., at a point at which in the absence of NADPH the steady-state level had been reached, shows that Cpd II formation is completely suppressed and/or reversed at ~10 μM NADPH, a concentration equimolar to that of the active heme centers (Figure 2b).[11,17]

Inhibition of Ascorbate-Induced Formation of Cpd II by $NADP^+$ and Thio-$NADP^+$. The recent finding that the $NADP^+$ produced upon reduction of Cpd I by tightly bound NADPH remains bound to the enzyme pocket[27] suggested that in the presence of $NADP^+$ Cpd I should also be protected against one-electron reduction by added ascorbic acid. In fact, the level of formation of Cpd II was increasingly diminished with increasing concentrations of $NADP^+$ (Figure 3a), as would be expected for a specific, competitive binding of $NADP^+$ and ascorbate. Complete suppression was achieved at ~100 μM, i.e., at a level 10-fold higher than that found for NADPH (see Figure S3 of the Supporting Information). This finding agrees well with earlier reports that NADPH binds more strongly to catalase than does $NADP^+$.[11,27,28] The data of Figure 3a suggested that addition of $NADP^+$ would lead to retardation of the ascorbate-induced Cpd I decay; i.e., a time depencence similar to that of the blank experiment in the absence of ascorbate (Figure 3b, top trace) was finally expected. Somewhat surprisingly, however, we found that simultaneous addition of $NADP^+$ and ascorbate even slightly enhanced the rate of decay of Cpd I in a concentration-dependent manner, following a sigmoid time dependence (Figure 3b).

Simultaneous monitoring of the absorption of ferricatalase at 405 nm (λ_{max}) in the foregoing experiments showed that the regeneration of ferricatalase mirrors the decay of Cpd I (Figure 3c). As observed previously for BLC and PMC,[28,43] in the absence of external reductants most of the Cpd I was reconverted (by the endogenous donor) to ferricatalase, and only a minor fraction, ~10–20%, was reduced to Cpd II, which is evident from the absorbance–time profiles monitored for the first 60 s after addition of peroxoacetic acid (compare Figures 2a and 3a). Even in the presence of 300 μM ascorbic acid, Cpd II still represented the smaller fraction (20–30%) of the Cpd I-derived products. In accord with the decay profile of Cpd I in Figure 3b, the formation of ferricatalase proceeded faster and to a higher degree when $NADP^+$ was added simultaneously with ascorbic acid. Although the ascorbate-dependent formation of Cpd II could be completely suppressed at ≥100 μM $NADP^+$, no full regeneration of ferricatalase was observed, as can be deduced from comparison of the limiting absorbances at 300 s with the initial absorbances prior to addition of peroxoacetic acid (see Figure 3b,c). The "missing" fraction of ~10% is tentatively attributed to degradation of the heme structures to products like biliverdin, which absorb above 600 nm.[53]

Further support for the blocking mode of inhibition of ascorbate-induced formation of Cpd II by $NADP^+$ was sought by employing thio-$NADP^+$, the nicotinic thiocarbamide analogue of $NADP^+$.[54,55] Thio-$NADP^+$ has a somewhat higher redox potential (−0.25 vs −0.32 V at pH 7)[56] and may adopt somewhat different binding conformations of the nicotinic amide group than $NADP^+$[57] but can be assumed to bind to the NADPH binding pocket with a strength similar to that of $NADP^+$. Thus, in case of a significant contribution of $NADP^+$ → NADPH reduction to the decay of Cpd I, a measurable difference in the concentration dependence was expected. However, thio-$NADP^+$ inhibited Cpd II formation to essentially the same degree as $NADP^+$ did (Figure S4a of the Supporting Information), achieving complete inhibition at ~100 μM (see Figure S4b of the Supporting Information). The data of Figure 3a thus support the conclusion that inhibition of formation of Cdp II by $NADP^+$ is a consequence of competitive docking.

To mimic a physiological situation more closely, the ascorbate-mediated formation of Cp II of BLC (2.5 μM) was also monitored under conditions of continuous generation of Cpd I from a low, constant flux of H_2O_2 generated by the glucose (10 mM)/glucose oxidase (2 nM) system. In the

dx.doi.org/10.1021/bi2017602 | Biochemistry 2012, 51, 4693–4703

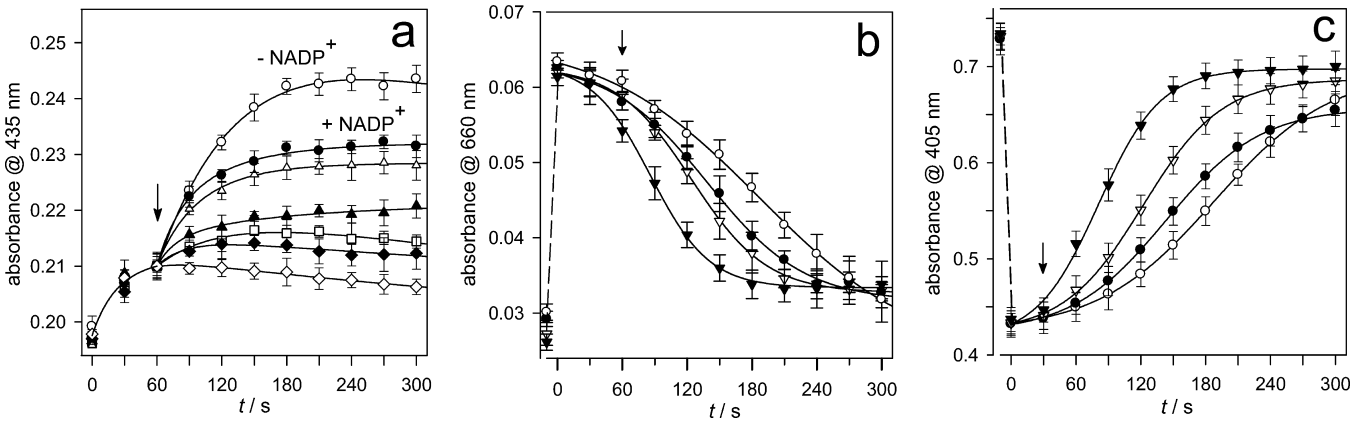

Figure 3. (a) Effect of $NADP^+$ on the formation of Cpd II from reaction of NADPH-free BLC (2.5 μM) with peroxoacetic acid (30 μM) in phosphate buffer (pH 7.4) at 25 °C, monitored at 435 nm (λ_{max}). Sixty seconds after the reactants had been mixed, only ascorbic acid (300 μM) (○) or ascorbic acid (300 μM) and increasing amounts of $NADP^+$ were simultaneously added. Final concentrations of $NADP^+$ were 1.0 (●), 2.5 (△), 10.0 (▲), 25.0 (□), 100 (◆), and 300 μM (◇). The solid lines (empirical exponential fits) are just intended to guide the eye. (b) Time dependence of the UV−vis absorption of Cpd I at 660 nm (λ_{max}) from the reaction of NADPH-free BLC (2.5 μM) with peroxoacetic acid (30 μM) in phosphate buffer (pH 7.4) at 25 °C, in the absence of any additives (○), in the presence of 300 μM ascorbic acid (●), in the presence of 300 μM ascorbic acid and 25 μM $NADP^+$ (▽), and in the presence of 300 μM ascorbic acid and 100 μM $NADP^+$ (▼). Solid lines show empirical least-squares fits to a sigmoidal function. (c) Time dependence of the UV−vis absorption of ferricatalase at 405 nm (λ_{max}) from the reaction of NADPH-free BLC (2.5 μM) with peroxoacetic acid (30 μM) in phosphate buffer (pH 7.4) at 25 °C, in the absence of any additives (○), in the presence of 300 μM ascorbic acid (●), in the presence of 300 μM ascorbic acid and 25 μM $NADP^+$ (▽), and in the presence of 300 μM ascorbic acid and 100 μM $NADP^+$ (▼). Solid lines show empirical least-squares fits to a sigmoidal function. In all figures, the arrow marks the point of addition of ascorbic acid and $NADP^+$. Data points before time zero show absorption prior to addition of peroxoacetic acid.

presence of 300 μM ascorbic acid, the buildup of Cpd II absorption proceeded exponentially, approaching a constant level within 20 min (Figure 4). In the presence of 20 μM $NADP^+$ or thio-$NADP^+$, the level of Cpd II production was reduced by ∼60% and largely suppressed at 5 mM, in correspondence with the observations made with peroxoacetic acid.

Inhibition of Ascorbate-Induced Formation of Cpd II by NADH and NAD^+. As mentioned in the introductory section, the binding of NADH to Clade 3 catalases is slightly less effective than binding of NADPH, and NAD^+ is the least strongly bound nucleotide.[11,27,28] This order was confirmed to be true in the presence of excess ascorbate, too (Figure 5). Measurable suppression of formation of Cpd II by NAD^+ was only observed at concentrations of ≥25 μM. Approximately 300 μM NAD^+ were required to achieve an inhibition level

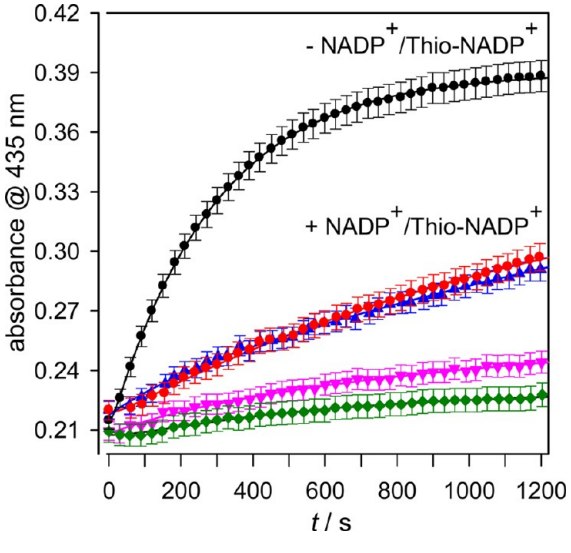

Figure 4. Formation of Cpd II from NADPH-free BLC (2.5 μM) in the presence of a glucose (10 mM)/glucose oxidase (2 nM) system and ascorbic acid (300 μM) in phosphate buffer (pH 7.4) at 25 °C, in the absence of any additives (●) and in the presence of 25 μM $NADP^+$ (red circles), 25 μM thio-$NADP^+$ (blue triangles), 1 mM $NADP^+$ (magenta triangles), and 5 mM $NADP^+$ (green diamonds). Solid lines are least-squares fits to a single-exponential equation.

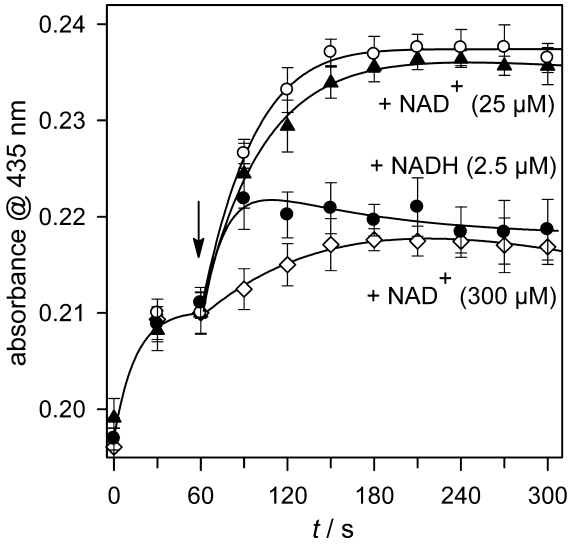

Figure 5. Effect of NADH and NAD^+ on the UV−vis absorption at 435 nm (λ_{max}) of Cpd II from reaction of NADPH-free BLC (2.5 μM) with peroxoacetic acid (30 μM) in phosphate buffer (pH 7.4) at 25 °C. Sixty seconds after the reactants had been mixed, ascorbic acid (300 μM) (○) or ascorbic acid (300 μM) and NADH or NAD^+ were simultaneously added (arrow). Final concentrations of NAD^+ were 25 (▲) and 300 μM (◇); the final concentration of NADH was 2.5 μM (●). The solid lines (empirical exponential fits) are just intended to guide the eye.

dx.doi.org/10.1021/bi2017602 | *Biochemistry* 2012, 51, 4693−4703

similar to that observed with 2.5 μM NADH or 25 μM $NADP^+$ (see Figure 3a). Thus, under these conditions, NAD^+ is ~10 times less effective than $NADP^+$ and ~100 times less effective than NADH in inhibiting Cpd II formation. From comparison with the data of Figure 2, the binding strength of NADH is estimated to be ~1.2−2 times smaller than that of NADPH, which is very consistent with a ratio of ~1.5 from previous estimates.[27,28]

Failure of Ascorbate To Induce Formation of Cpd II from *A. niger* (Clade 2) Catalase. Catalase from *A. niger* (ANC) is a Clade 2 catalase that does not bind NADPH as a cofactor. It has been reported that Cpd II can barely be detected when ANC is treated with alkyl hydroperoxides,[48,58,59] suggesting that initially formed Cpd I is not effectively converted to Cpd II by the endogenous donor.[48] Likewise, the spectrum of Cpd I of ANC has briefly been mentioned not to be affected by 5 mM external ascorbate.[58] However, slow formation of Cpd II of ANC has been observed in the presence of the H_2O_2-generating glucose/glucose oxidase system at pH 3.5.[49,60] Cpd II of ANC can also be produced by the unspecific one-electron reductant hexacyanoferrate(II).[61] Thus, if only specific binding of ascorbate to an existing NADPH pocket would allow one-electron reduction of Cpd I, no buildup of Cpd II should be observable from ANC and the glucose/glucose oxidase system in the presence of ascorbate. This indeed turned out to be the case, as demonstrated in Figure 6 by comparison with BLC.

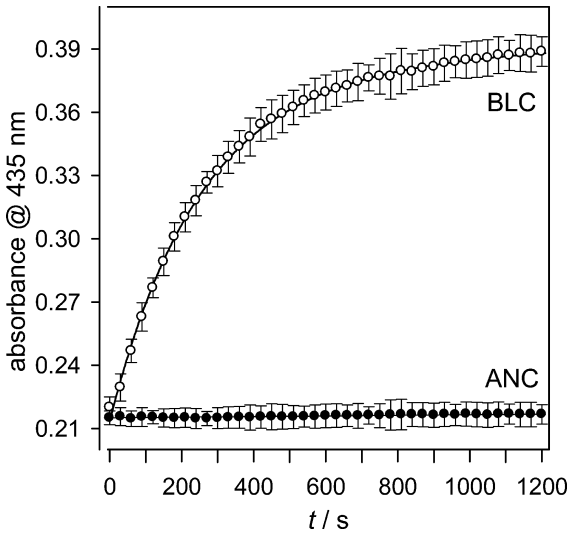

Figure 6. Formation of Cpd II from NADPH-free BLC (2.5 μM) (○) and from NADPH-free *A. niger* catalase (ANC; 2.5 μM) (●) in the presence of a glucose (10 mM)/glucose oxidase (2 nM) system and ascorbic acid (300 μM) in phosphate buffer (pH 7.4) at 25 °C. Solid lines are least-squares fits to a single-exponential equation.

Molecular Mechanics Docking Computations of Dinucleotide and Ascorbate Binding. To gain deeper insight into the structural characteristics of $NADPH/NADP^+$ and $AscH^-$ binding, molecular mechanics (MM) docking computations were conducted. For several NADPH-free and NADPH-bound Clade 3 catalases, X-ray structures are available from the PDB.[62] These data reveal a highly conserved amino acid sequence for the binding pockets of the various catalases. It is noteworthy that, by comparison of the PDB data with X-ray structural data of various dihydronicotinamide/nicotinamide derivatives,[63−67] it appears that in all published NADPH-bound catalase structures the bound dinucleotide is in fact the oxidized form, $NADP^+$. The experimental structure of the NADPH binding pocket of HEC with bound $NADP^+$ is shown in Figure 7a.

As discussed previously,[1,2] a unique feature of the bound $NADP^+/NADPH$ is the unusually helical conformation, which allows both the nicotinamide and adenine group to deeply penetrate the protein pocket and have a short mutual distance. We recognize, as characteristic stabilizing forces, π-stacking interactions of the perpendicularly oriented adenine group with arginine and phenylalanine residues Arg203 and Phe198 and hydrogen bond-assisted ionic (Coulomb) interactions of the doubly negatively charged ribose 2′-phosphate group with the positively charged arginine (Arg203) and lysine (Lys237) residues. As a consequence of this binding motif, the nicotinamide group is located at the entrance of the "right" branch of the lateral channel (see Figure 7a), i.e., the one that has been proposed to be the major pathway for the flow of electrons from NADPH,[29] whereas the second, "left", branch is blocked by the adenine−ribose tail.

The computed minimal structures of the pocket-bound complexes of $NADP^+$ (Figure 7b) and NADPH (Figure S7a of the Supporting Information) show a very similar arrangement, indicating that the binding interactions mentioned above are well reflected by the computations. As expected, NADH shows a very similar binding motif (Figure S7b of the Supporting Information) despite the fact that the ionic interactions of the ribose 2′-phosphate group with Arg203 and Lys237 are missing. On the other hand, and in agreement with its weak protective effect against Cpd II formation, pocket binding of NAD^+ was predicted to be unfavorable, because on optimization NAD^+ is forced out of the cavity to finally remain associated with residue Lys306 at the surface of the protein (Figure S7d of the Supporting Information).

Interestingly, the optimization also revealed a $NADP^+$ complex in which the nicotinamide moiety is completely rotated out of the binding pocket, but with the adenine tail remaining firmly fixed in its place (Figure S7c of the Supporting Information). The "out" bound structure of $NADP^+$ is predicted to be only 5 kJ mol^{-1} higher in energy than the "in" bound structure. Noteworthy, an "out" bound structure was not found for NADPH; upon optimization of "out" starting structures, the system always returned to the fully bound state as depicted in Figure S7a of the Supporting Information.

The optimization of the various ascorbate complexes (one to four $AscH^-$ molecules initially placed in the pocket) showed only one $AscH^-$ unit remained deeply buried in the pocket, occupying the adenine-binding site between the positive Arg203 and Phe198 residues (Figure 7c). A second $AscH^-$ occupies the gap between the Arg203 and Lys237 residues at the surface of the protein, whereas a third and fourth ascorbate are predicted to fully leave the pocket and to remain associated with a positive surface residue.

DISCUSSION

Background. The spectroscopic detection of intermediates Cpd I, Cpd II, and Cpd III in the late 1940s[30−34,68] was the major breakthrough in the understanding of the mechanism of the catalase reaction (and that of other heme enzymes). A further facet to the complexity of the catalase reaction was added by the landmark discovery of specific binding of NADPH as a cofactor in Clade 3 (mammalian) catalases.[11] It is now

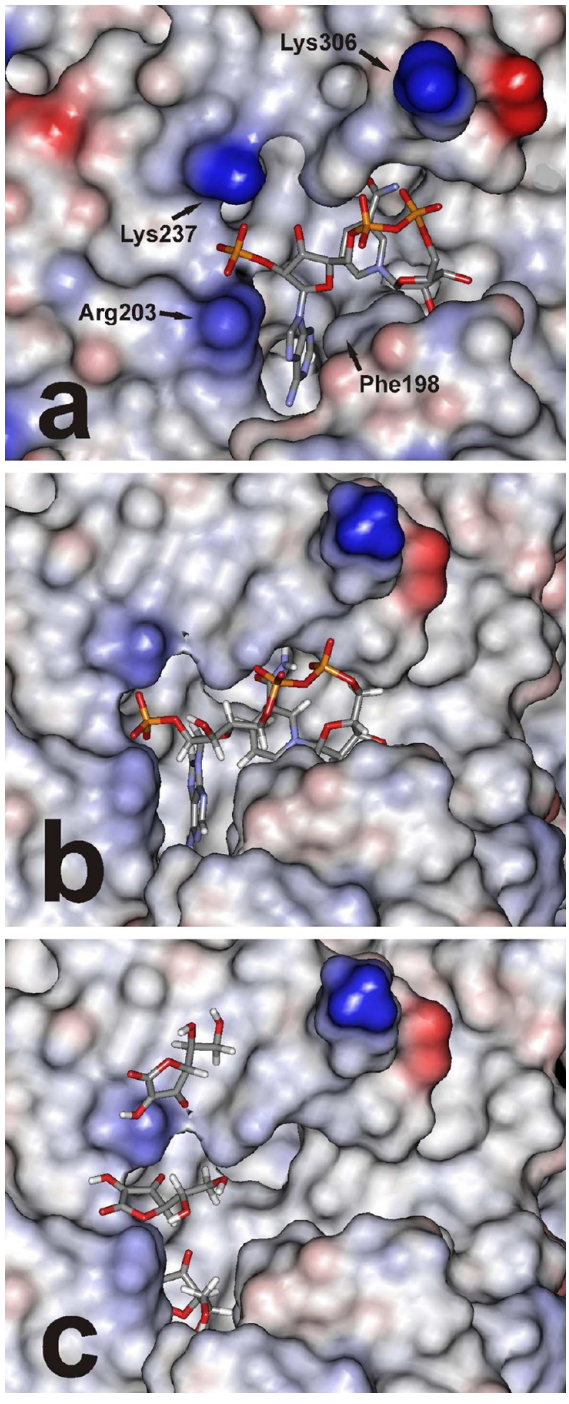

Figure 7. (a) Experimental X-ray structure (water molecules omitted) of the NADPH binding pocket of HEC (PDB entry 1DGF, subunit A) with $NADP^+$ bound, showing the entrances to the nicotinamide (right) and adenine- and ribose-occupied (left) branches of the lateral channel to the heme center. (b) MM-optimized structure, with H atoms added, of the HEC binding pocket with "in" bound $NADP^+$. (c) MM-optimized structure of the HEC binding pocket with three bound ascorbate ($AscH^-$) molecules. Protein coloring denotes the electrostatic potential (blue for positive, red for negative).

generally accepted that NADPH (as well as NADH) serves as a protective factor for these catalases, preventing self-oxidation of the protein by the key intermediate Cpd I with formation of the catalytically inactive species Cpd II.

Formation of Cpd I of catalases from reaction with hydrogen peroxide, alkyl hydroperoxides, or peroxo acids, decay of Cpd I, formation of Cpd II by one-electron reduction, and the effect of $NAD(P)H/NAD(P)^+$ on both intermediates have been quite intensely investigated. The previous findings are generally confirmed in this study. As major characteristics we note that (i) the decay of Cpd I by action of the endogenous donor, i.e., in the absence of any external reductant, leads chiefly to regeneration of ferricatalase but only to modest formation of Cpd II and (ii) Cpd I and Cpd II can hardly be detected in the presence of NADPH. Even in the early spectroscopic studies of catalase intermediates, the conversion of the key intermediate Cpd I to Cpd II by added ascorbic acid had been exploited.[30,31,51,69,70] The reduction of Cpd I by ascorbate has been repeatedly observed in the past, but detailed studies of the pathways of electron/proton flow can hardly be found. Prior to the first X-ray studies of mammalian catalases, (see ref 29 for references) that revealed that the substrate channel to the deeply embedded heme centers would be too narrow to allow effective ascorbate transportation, the effect of ascorbic acid/ascorbate on catalases was generally assumed to be due to more or less direct interaction with the heme iron. The presence of a minor (lateral), bifurcated channel, i.e., the one that is blocked by NADPH in Clade 3 catalases, later led to the suggestion that this channel would allow inhibitors to access the active site.[2]

It should be remembered that the inertness of Cpd II against further reduction by ascorbate is a characteristic feature of catalases. Forms of Cpd II of other heme enzymes, e.g., ascorbate peroxidase,[71,72] cytochrome c peroxidase,[73] or myeloperoxidase,[74] are effectively reduced by ascorbate.

NADPH versus Ascorbate Pocket Binding. In this study, we provide evidence that one-electron reduction of Cpd I to Cpd II by ascorbate proceeds solely via binding of ascorbate to the NADPH binding pocket. From Figure 2, it is evident that the $AscH^-$-mediated Cpd I → Cpd II conversion is essentially completely suppressed at a NADPH concentration equimolar to the concentration of the active heme sites, indicating a strong association of NADPH. In fact, the specific pocket binding of NADPH to Clade 3 catalases is extremly tight. From the limiting values of dissociation constant $K_D(NADPH)$ of ≤10 and ≤5 nM for binding of NADPH to BLC and PMC,[11,17,75] respectively, a binding free energy $[\Delta_B G^\circ(NADPH)]$ of ≤−11 kcal mol^{-1} can be estimated. The dissociation constant of the $AscH^-$−BLC complex $[K_D(AscH^-)]$ has recently been reported to be 44 μM.[39] This corresponds to a binding strength $[\Delta_B G^\circ(AscH^-)]$ of −5.9 kcal mol^{-1}. Thus, there is a difference in the specific binding strength $(\Delta\Delta G^\circ)$ of approximately ≤−5 kcal mol^{-1} in favor of NADPH; i.e., NADPH outcompetes $AscH^-$ for pocket binding. From the difference in binding strengths, it can further be estimated that substantial exchange of pocket-bound NAD(P)H by ascorbate would be important only at very high concentrations (≥40 mM) of ascorbate (see below).

$NADP^+$ versus Ascorbate Binding. In accord with the finding that $NADP^+$ remains bound to the pocket,[11,27,28] ascorbate-mediated Cp II formation is also suppressed by added $NADP^+$, but a 10-fold higher concentration versus that for NADPH is needed to achieve comparable protection (see Figure 3a and Figure S3 of the Supporting Information; for easier comparison, related time dependencies for NADPH, NADH, $NADP^+$, and NAD^+ are summarized in Figure S5 of the Supporting Information). An almost identical concentration dependence was found for thio-$NADP^+$ (Figure S4 of the

dx.doi.org/10.1021/bi2017602 | *Biochemistry* 2012, 51, 4693−4703

Supporting Information). The NADPH:NADP$^+$ concentration ratio of 1:10 is in excellent agreement with previous reports of the related binding strengths. For comparison, Kirkman et al. found a molar NADPH:NADP$^+$ ratio of ∼12−13:1 for binding to BLC.[11]

The unexpected finding that in the presence of NADP$^+$ the ascorbate-induced decay of Cpd I is slightly enhanced rather that retarded (Figure 3b), but that ferricatalase regeneration is similarly enhanced (Figure 3c), demands further investigation. The reasonable explanation that such a behavior might simply be due to (partial) reduction of NADP$^+$(bound) to NADPH-(bound) by ascorbate can, however, be ruled out because the redox potentials at pH 7 of the AscH$^-$/DHA [$E^{o\prime}$(AscH$^-$/DHA) = 0.48 V[76]], AscH$^-$/Asc$^{\bullet-}$ [$E^{o\prime}$(AscH$^-$/Asc$^{\bullet-}$) = 0.33 V[77]], and Asc$^{\bullet-}$/DHA [$E^{o\prime}$(Asc$^{\bullet-}$/DHA) = 0.24 V[76]] couples are all more positive than that of the NAD(P)$^+$/NAD(P)H couple [$E^{o\prime}$(NAD$^+$/NADH) = −0.315 V; $E^{o\prime}$(NADP$^+$/NADPH) = −0.324 V[78]]. Thus, NAD(P)H is a stronger reductant than AscH$^-$, making reduction of NADP$^+$ by AscH$^-$ highly unfavorable.

NADH/NAD$^+$ versus Ascorbate Binding. Clear evidence of blocking of specific binding of ascorbate by NADP$^+$ is provided by the effects of NADH/NAD$^+$ on Cdp II formation (Figure 5). Our data demonstrate that NADH is only 1.2−2 times less effective than NADPH in the suppression of Cpd II formation, in excellent agreement with the relative strengths of binding of both dinucleotides to the enzyme pocket.[11,27,28] On the other hand, NAD$^+$ is found to be ∼100 and ∼10 times less effective than NADPH/NADH and NADP$^+$, respectively. Because the electrochemical potentials of NADH/NAD$^+$ and NADPH/NADP$^+$ redox couples are essentially identical (see above), a similar activity of NAD$^+$ as observed for NADP$^+$ would be expected in the case of substantial reduction to NADH. As seen in Figures 3a and 5 and Figure S5 of the Supporting Information, this is not the case. A 10-fold higher concentration of NAD$^+$ compared to that of NADH induces only a small protective effect. Thus, if only 10% of the applied NAD$^+$ would be reduced to NADH, a similar inhibition of Cpd II as observed for 2.5 μM NADH would be expected. In conclusion, for both the reduced and oxidized forms of the nucleotides, sterical blocking of ascorbate binding is the major, if not the only, operating protection mechanism.

Conclusions from the Docking Computations. As noted above, the experimental pocket binding of NADP$^+$/NADPH (Figure 7a) is reproduced well in the MM docking computations (Figure 7b and Figure S7a of the Supporting Information). The interesting finding of a NADP$^+$ complex with the nicotinamide−ribose tail pointing out of the pocket (Figure S7c of the Supporting Information) agrees with the experimental observation that NADP$^+$, once formed from bound NADPH, remains bound to the pocket and is not replaced by external NADPH.[27] In line with strong hydrogen bond-assisted ionic interactions, ascorbate was predicted to be preferably bound to residues Arg203 and Lys237, i.e., occupying the left branch of the lateral channel (Figure 7c). Stable binding of AscH$^-$ in other regions of the pocket was not found; additional AscH$^-$ molecules were forced out of the pocket, which can be attributed to mutual charge repulsion of the ascorbate anions as well as a hydrophobic character of the pocket at the entrance to the right branch of the lateral channel. This finding would explain why NADP$^+$ is effective in suppressing ascorbate binding, and thus Cpd II formation, even if its nicotiniumamide tail would be oriented outward (Figure S7c of the Supporting Information).

It is interesting to note that the same dominating interactions for binding of ascorbate, i.e., with positively charged arginine and lysine residues, are also found in ascorbate peroxidase.[79]

Biological Implications. What are the biological consequences of the findings presented here? The interaction of catalases with ascorbic acid/ascorbate has been studied since the 1930s, and in most cases, inhibitory effects have been reported. On pages S8−S12 of the Supporting Information, we mention a number of studies of the effect of ascorbic acid on the in vitro and in vivo activity of catalases. These studies now must be examined in light of our findings. For instance, because NADPH, NADH, and even NADP$^+$ are strongly bound to mammalian catalases, we must suspect that in a number of isolations of Clade 3 catalases a fraction or even all of the available binding sites could have been loaded with these nucleotides,[11] depending on the isolation protocol. Hence, studies of the interaction of ascorbic acid with Clade 3 catalases may have been variably affected by bound cofactors. This would, at least in part, explain the sometimes contradictory observations with regard to the inhibitory effects of ascorbate. On the other hand, with regard to a competition of NAD(P)H and ascorbate on catalase activity in physiological systems, which would negatively affect the antioxidative defense system, it is evident that as long as normal, physiological levels of NAD(P)H level are maintained, no noticeable inhibition of catalase by ascorbate must be expected, because typical levels of ascorbate are well below the limiting value of ∼40 mM.[80,81]

Reports of specific binding of bioactive molecules other than ascorbate to mammalian catalases have also been published (see page S12 of the Supporting Information for examples). Considering the observations made here for ascorbic acid/ascorbate, we strongly suggest that in studies focused on the interaction of Clade 3 catalases with (potentially) bioactive compounds the presence of NADPH/NADP$^+$ should be established, and the effect of supplementation of these dinucleotides must not be neglected.

■ ASSOCIATED CONTENT

Supporting Information

Normalized visible spectra of Cpd I of Clade 3 catalases from various sources, the time dependence of the visible spectrum (500−800 nm) of Cpd I of BLC, absorption intensities of Cpd II as a function of NADP$^+$ and thio-NADP$^+$ concentration, structures of the DFT-computed conformers of AscH$^-$, graphical presentations of the NADPH-binding region of HEC with bound NADPH, NADH, NADP$^+$, and NAD$^+$ from MM docking computations, and a collection of references concerning the effect of specifing binding ascorbate and other molecules on catalase activity. This material is available free of charge via the Internet at http://pubs.acs.org.

■ AUTHOR INFORMATION

Corresponding Author

*H.-G.K.: Institut für Organische Chemie, Universität Duisburg-Essen, Universitätsstrasse 5, 45117 Essen, Germany; phone, (++49)201-183-3148; fax, (++49)201-183-4259; e-mail, hans-gert.korth@uni-duisburg-essen.de. M.K.: Institut für Physiologische Chemie, Universitätsklinikum Essen, Hufelandstr. 52, 45122 Essen, Germany; e-mail, michael.kirsch@uni-duisburg-essen.de.

Notes

The authors declare no competing financial interest.

■ ABBREVIATIONS

BLC, bovine liver catalase; HEC, human erythrocyte catalase; ANC, *A. niger* catalase; PMC, *Proteous mirabilis* catalase; SCC-A, *Saccharomyces cerevisiae* catalase A; Cpd I, Compound I; Cpd II, Compound II; $AscH_2$, ascorbic acid; $AscH^-$, ascorbate or ascorbic acid monoanion; $Asc^{\bullet-}$, ascorbyl radical anion; DHA, dehydroascorbic acid; NADPH, reduced nicotinamide adenine dinucleotide phosphate; $NADP^+$, oxidized nicotinamide adenine dinucleotide phosphate; NADH, reduced nicotinamide adenine dinucleotide; NAD^+, oxidized nicotinamide adenine dinucleotide; thio-$NADP^+$, oxidized thio-nicotinamide adenine dinucleotide phosphate; DTPA, diethylenetriaminepentaacetic acid; MM, molecular mechanics.

■ ADDITIONAL NOTE

[a]From this value, an apparent second-order rate constant (k_{app}) of 73 M^{-1} s^{-1} for the Cpd I–$AscH^-$ reaction is estimated. Chance[30] had reported a rate constant for horse blood catalase (HBC) that was ~4 times higher (k_{app} = 360 M^{-1} s^{-1}) from monitoring the Soret band at 405 nm (λ_{max}). However, with regard to the complexity of the reduction mechanism, derivation of a second-order rate constant is questionable.

■ REFERENCES

(1) Zamocky, M., and Koller, F. (1999) Understanding the structure and function of catalases: Clues from molecular evolution and in vitro mutagenesis. *Prog. Biophys. Mol. Biol. 72*, 19–66.

(2) Nicholls, P., Fita, I., and Loewen, P. C. (2001) Enzymology and structure of catalases. *Adv. Inorg. Chem. 51*, 51–106.

(3) Schonbaum, G. R., and Chance, B. (1976) Catalase. In *The Enzymes* (Boyer, P. D., Ed.) 3rd ed., pp 363–408, Academic Press, New York.

(4) Deisseroth, A., and Dounce, A. L. (1970) Catalase: Physical and chemical properties, mechanism of catalysis, and physiological role. *Physiol. Rev. 50*, 319–375.

(5) Nicholls, P., and Schonbaum, G. R. (1963) Catalases. In *The Enzymes* (Boyer, P. D., Lardy, H., and Myrbäck, K., Eds.) 2nd ed., pp 147–225, Academic Press, New York.

(6) Maté, M. J., Murshudov, G., Bravo, J., Melik-Adamyan, W., Loewen, P. C., and Fita, I. (2001) Heme-catalases. In *Handbook of Metalloproteins* (Messerschmidt, A., Huber, R., Poulos, T., and Wieghardt, K., Eds.) pp 486–502, Wiley, Chichester, U.K.

(7) Chelikani, P., Fita, I., and Loewen, P. C. (2004) Diversity of structures and properties among catalases. *Cell. Mol. Life Sci. 61*, 192–208.

(8) Zamocky, M., Furtmueller, P. G., and Obinger, C. (2008) Evolution of catalases from bacteria to humans. *Antioxid. Redox Signaling 10*, 1527–1548.

(9) Kirkman, H. N., and Gaetani, G. F. (2007) Mammalian catalase: A venerable enzyme with new mysteries. *Trends Biochem. Sci. 32*, 44–50.

(10) Jones, P. (2010) Catalases. In *Peroxidases & Catalases* (Dunford, H. B., Ed.) 2nd ed., pp 233–256, Wiley, Hoboken, NJ.

(11) Kirkman, H. N., and Gaetani, G. F. (1984) Catalase: A tetrameric enzyme with four tightly bound molecules of NADPH. *Proc. Natl. Acad. Sci. U.S.A. 81*, 4343–4347.

(12) Fita, I., and Rossmann, M. G. (1985) The NADPH binding site on beef liver catalase. *Proc. Natl. Acad. Sci. U.S.A. 82*, 1604–1608.

(13) Ko, T. P., Day, J., Malkin, A. J., and McPherson, A. (1999) Structure of orthorhombic crystals of beef liver catalase. *Acta Crystallogr. D55*, 1383–1394.

(14) Murshudov, G. N., Grebenko, A. I., Brannigan, J. A., Antson, A. A., Barynin, V. V., Dodson, G. G., Dauter, Z., Wilson, K. S., and Melik-Adamyan, W. R. (2002) The structures of *Micrococcus lysodeikticus* catalase, its ferryl intermediate (compound II) and NADPH complex. *Acta Crystallogr. D58*, 1972–1982.

(15) Gouet, P., Jouve, H.-M., and Dideberg, O. (1995) Crystal structure of *Proteus mirabilis* PR catalase with and without bound NADPH. *J. Mol. Biol. 249*, 933–954.

(16) Putnam, C. D., Arvai, A. S., Bourne, Y., and Tainer, J. A. (2000) Active and inhibited human catalase structures: Ligand and NADPH binding and catalytic mechanism. *J. Mol. Biol. 296*, 295–309.

(17) Kirkman, H. N., Galiano, S., and Gaetani, G. F. (1987) The function of catalase-bound NADPH. *J. Biol. Chem. 262*, 660–666.

(18) Hillar, A., and Nicholls, P. (1992) A mechanism for NADPH inhibition of catalase compound II formation. *FEBS Lett. 314*, 179–182.

(19) Almarsson, O., Sinha, A., Gopinath, E., and Bruice, T. C. (1993) Mechanism of one-electron oxidation of NAD(P)H and function of NADPH bound to catalase. *J. Am. Chem. Soc. 115*, 7093–7102.

(20) Hillar, A., Nicholls, P., Switala, J., and Loewen, P. C. (1994) NADPH binding and control of catalase compound II formation: Comparison of bovine, yeast, and *Escherichia coli* enzymes. *Biochem. J. 300*, 531–539.

(21) Cattani, L., and Ferri, A. (1994) The function of NADPH bound to catalase. *Boll.—Soc. Ital. Biol. Sper. 70*, 75–82.

(22) Olson, L. P., and Bruice, T. C. (1995) Electron tunneling and ab initio calculations related to the one-electron oxidation of NAD(P)H bound to catalase. *Biochemistry 34*, 7335–7347.

(23) Bicout, D. J., Field, M. J., Gouet, P., and Jouve, H. M. (1995) Simulations of electron transfer in the NADPH-bound catalase from *Proteus mirabilis* PR. *Biochim. Biophys. Acta 1252*, 172–176.

(24) Kirkman, H. N., Rolfo, M., Ferraris, A. M., and Gaetani, G. F. (1999) Mechanisms of protection of catalase by NADPH. Kinetics and stoichiometry. *J. Biol. Chem. 274*, 13908–13914.

(25) Alfonso-Prieto, M., Borovik, A., Carpena, X., Murshudov, G., Melik-Adamyan, W., Fita, I., Rovira, C., and Loewen, P. C. (2007) The Structures and Electronic Configuration of Compound I Intermediates of *Helicobacter pylori* and *Penicillium vitale* Catalases Determined by X-ray Crystallography and QM/MM Density Functional Theory Calculations. *J. Am. Chem. Soc. 129*, 4193–4205.

(26) Horner, O., Mouesca, J. M., Solari, P. L., Orio, M., Oddou, J. L., Bonville, P., and Jouve, H. M. (2007) Spectroscopic description of an unusual protonated ferryl species in the catalase from *Proteus mirabilis* and density functional theory calculations on related models. Consequences for the ferryl protonation state in catalase, peroxidase and chloroperoxidase. *J. Biol. Inorg. Chem. 12*, 509–525.

(27) Gaetani, G. F., Ferraris Anna, M., Sanna, P., and Kirkman, H. N. (2005) A novel NADPH:(bound)$NADP^+$ reductase and NADH:(bound)$NADP^+$ transhydrogenase function in bovine liver catalase. *Biochem. J. 385*, 763–768.

(28) Jouve, H. M., Pelmont, J., and Gaillard, J. (1986) Interaction between pyridine adenine dinucleotides and bovine liver catalase: A chromatographic and spectral study. *Arch. Biochem. Biophys. 248*, 71–79.

(29) Sicking, W., Korth, H.-G., de Groot, H., and Sustmann, R. (2008) On the functional role of a water molecule in clade 3 catalases: A proposal for the mechanism by which NADPH prevents the formation of compound II. *J. Am. Chem. Soc. 130*, 7345–7356.

(30) Chance, B. (1947) An intermediate compound in the catalase-hydrogen peroxide reaction. *Acta Chem. Scand. 1*, 236–267.

(31) Lemberg, R., and Foulkes, E. C. (1948) Reaction between catalase and hydrogen peroxide. *Nature 161*, 131–132.

(32) Chance, B. (1949) The primary and secondary compounds of catalase and methyl or ethyl hydrogen peroxide. I. Spectra. *J. Biol. Chem. 179*, 1331–1339.

(33) Chance, B. (1950) Reactions of catalase in the presence of the notatin system. *Biochem. J. 46*, 387–402.

(34) Keilin, D., and Hartree, E. F. (1951) Purification of horseradish peroxidase and comparison of its properties with those of catalase and methemoglobin. *Biochem. J. 49*, 88–104.

(35) Chance, B. (1952) Catalase and peroxides. I. The spectra of enzyme-substrate complexes of catalase and peroxidase. *Arch. Biochem. Biophys. 41*, 404−415.
(36) Stern, K. G. (1936) The mechanism of enzyme action. A study of the decomposition of ethyl hydrogen peroxide by catalase and of an intermediate enzyme-substrate compound. *J. Biol. Chem. 114*, 473−494.
(37) Stern, K. G. (1937) Spectrography of the reaction of catalase with ethyl hydrogen peroxide. *Enzymologia 4*, 145−147.
(38) Keilin, D., and Nicholls, P. (1958) Reactions of catalase with hydrogen peroxide and hydrogen donors. *Biochim. Biophys. Acta 29*, 302−307.
(39) Li, D., Ji, B., and Jin, J. (2008) Spectrophotometric studies on the binding of vitamin C to lysozyme and bovine liver catalase. *J. Lumin. 128*, 1399−1406.
(40) Kirsch, M., and de Groot, H. (2000) Ascorbate is a potent antioxidant against peroxynitrite-induced oxidation reactions. Evidence that ascorbate acts by re-reducing substrate radicals produced by peroxynitrite. *J. Biol. Chem. 275*, 16702−16708.
(41) Samejima, N., and Yang, J. (1963) Reconstitution of acid-denaturated catalase. *J. Biol. Chem. 238*, 3256−3261.
(42) Gebicka, L., Metodiewa, D., and Gebicki, J. L. (1989) Pulse radiolysis of catalase in solution. I. Reactions of superoxide anion with catalase and its compound I. *Int. J. Radiat. Biol. 55*, 45−50.
(43) Andreoletti, P., Gambarelli, S., Sainz, G., Stojanoff, V., White, C., Desfonds, G., Gagnon, J., Gaillard, J., and Jouve, H. M. (2001) Formation of a tyrosyl radical intermediate in *Proteus mirabilis* catalase by directed mutagenesis and consequences for nucleotide reactivity. *Biochemistry 40*, 13734−13743.
(44) Jones, P., and Middlemiss, D. N. (1972) Formation of compound I by the reaction of catalase with peroxoacetic acid. *Biochem. J. 130*, 411−415.
(45) Frisch, M. J., et al. (2009) *Gaussian 09*, revision A.02, Gaussian, Inc., Wallingford, CT.
(46) Palcic, M. M., and Dunford, H. B. (1980) The reaction of human erythrocyte catalase with hydroperoxides to form compound I. *J. Biol. Chem. 255*, 6128−6132.
(47) Hara, I., Ichise, N., Kojima, K., Kondo, H., Ohgiya, S., Matsuyama, H., and Yumoto, I. (2007) Relationship between the Size of the Bottleneck 15 Å from Iron in the Main Channel and the Reactivity of Catalase Corresponding to the Molecular Size of Substrates. *Biochemistry 46*, 11−22.
(48) DeLuca, D. C., Dennis, R., and Smith, W. G. (1995) Inactivation of an animal and a fungal catalase by hydrogen peroxide. *Arch. Biochem. Biophys. 320*, 129−134.
(49) Lardinois, O. M., Mestdagh, M. M., and Rouxhet, P. G. (1996) Reversible inhibition and irreversible inactivation of catalase in presence of hydrogen peroxide. *Biochim. Biophys. Acta 1295*, 222−238.
(50) Ferri, A. (1990) Action of catalase on peroxoacetic acid. Kinetic studies. *Biochem. Int. 21*, 623−631.
(51) Chance, B. (1950) Reaction of catalase peroxides with acceptors. *J. Biol. Chem. 182*, 649−658.
(52) Nicholls, P. (1961) Action of anions on catalase-peroxide compounds. *Biochem. J. 81*, 365−374.
(53) Marko, H., Mueller, N., and Falk, H. (1989) Complex Formation Between Biliverdin and Apomyoglobin. *Monatsh. Chem. 120*, 591−596.
(54) Stein, A. M., Lee, J. K., Anderson, C. D., and Anderson, B. M. (1963) The thionicotinamide analogs of di- and triphosphopyridine nucleotide (DPN and TPN). I. Preparation and analysis. *Biochemistry 2*, 1015−1017.
(55) Anderson, B. M., Anderson, C. D., and Stein, A. M. (1963) Enzyme studies. *Biochemistry 2*, 1017−1022.
(56) Yakovlev, G., and Hirst, J. (2007) Transhydrogenation Reactions Catalyzed by Mitochondrial NADH-Ubiquinone Oxidoreductase (Complex I). *Biochemistry 46*, 14250−14258.
(57) Singh, A., Venning, J. D., Quirk, P. G., van Boxel, G. I., Rodrigues, D. J., White, S. A., and Jackson, J. B. (2003) Interactions between Transhydrogenase and Thio-nicotinamide Analogues of NAD(H) and NADP(H) Underline the Importance of Nucleotide Conformational Changes in Coupling to Proton Translocation. *J. Biol. Chem. 278*, 33208−33216.
(58) Kikuchi-Torii, K., Hayashi, S., Nakamoto, H., and Nakamura, S. (1982) Properties of *Aspergillus niger* catalase. *J. Biochem. 92*, 1449−1456.
(59) Kikuchi, K., Kawamura-Konishi, Y., and Suzuki, H. (1992) The reaction of *Aspergillus niger* catalase with methyl hydroperoxide. *Arch. Biochem. Biophys. 296*, 88−94.
(60) Lardinois, O. M., and Rouxhet, P. G. (1994) Characterization of hydrogen peroxide and superoxide degrading pathways of *Aspergillus niger* catalase: A steady-state analysis. *Free Radical Res. 20*, 29−50.
(61) Bruchmann, E. E., Haller, C. P., and Schneider, H. M. (1986) Effect of hexacyanoferrate(II) ions on citric acid fermentation. *Chem.-Ztg. 110*, 93−94.
(62) Protein Data Bank. http://www.rcsb.org/pdb/.
(63) Ishida, T., Miyamoto, Y., Nakamura, A., and Inoue, M. (1982) Structure of 1-[2-(adenin-9-yl)ethyl]-13-carbamoylpyridinium ($AC2N^+$) chloride monohydrate, a pyridine-coenzyme model. *Acta Crystallogr. B38*, 192−195.
(64) Glasfeld, A., Zbinden, P., Dobler, M., Benner, S. A., and Dunitz, J. D. (1988) Crystal structures of two simple N-substituted dihydronicotinamides: Possible implications for stereoelectronic arguments in enzymology. *J. Am. Chem. Soc. 110*, 5152−5157.
(65) Karle, I. L. (1961) The crystal structure of N-benzyl-1,4-dihydronicotinamide. *Acta Crystallogr. 14*, 497−502.
(66) Guillot, B., Muzet, N., Artacho, E., Lecomte, C., and Jelsch, C. (2003) Experimental and Theoretical Electron Density Studies in Large Molecules: NAD^+, β-Nicotinamide Adenine Dinucleotide. *J. Phys. Chem. B 107*, 9109−9121.
(67) Reddy, B. S., Saenger, W., Muehlegger, K., and Weimann, G. (1981) Crystal and molecular structure of the lithium salt of nicotinamide adenine dinucleotide dihydrate (NAD^+, DPN^+, cozymase, codehydrase I). *J. Am. Chem. Soc. 103*, 907−914.
(68) Chance, B. (1949) Properties of the enzyme-substrate compounds of peroxidase and peroxides. I. Spectra of the primary and secondary complexes. *Arch. Biochem. 21*, 416−430.
(69) Foulkes, E. C., and Lemberg, R. (1948) The inhibition of catalase by ascorbic acid. *Aust. J. Exp. Biol. Med. Sci. 26*, 307−313.
(70) Foulkes, E. C., and Lemberg, R. (1949) The azide inhibition of catalase. *Enzymologia 13*, 302−312.
(71) Raven, E. L. (2003) Understanding functional diversity and substrate specifity in haem peroxidases: What can we learn from ascorbate peroxidase? *Nat. Prod. Rep. 20*, 367−381.
(72) Efimov, I., Papadopoulou, N. D., McLean, K. J., Badyal, S. K., Macdonald, I. K., Munro, A. W., Moody, P. C. E., and Raven, E. L. (2007) The Redox Properties of Ascorbate Peroxidase. *Biochemistry 46*, 8017−8023.
(73) Marquez, L. A., Dunford, H. B., and Van Wart, H. (1990) Kinetic studies on the reaction of compound II of myeloperoxidase with ascorbic acid. Role of ascorbic acid in myeloperoxidase function. *J. Biol. Chem. 265*, 5666−5670.
(74) Murphy, E. J., Metcalfe, C. L., Basran, J., Moody, P. C. E., and Lloyd Raven, E. (2008) Engineering the Substrate Specificity and Reactivity of a Heme Protein: Creation of an Ascorbate Binding Site in Cytochrome c Peroxidase. *Biochemistry 47*, 13933−13941.
(75) Jouve, H. M., Beaumont, F., Leger, I., Foray, J., and Pelmont, J. (1989) Tightly bound NADPH in *Proteus mirabilis* PR catalase. *Biochem. Cell Biol. 67*, 271−277.
(76) Tur'yan, Y. I., and Kohen, R. (1995) Formal redox potentials of the dehydro-L-ascorbic acid/L-ascorbic acid system. *J. Electroanal. Chem. 380*, 273−277.
(77) Njus, D., and Kelley, P. M. (1991) Vitamins C and E donate single hydrogen atoms in vivo. *FEBS Lett. 284*, 147−151.
(78) Gossauer, A. (2006) *Struktur und Reaktivität der Biomoleküle*, p 232, Verlag Helvetica Chimica Acta, Zurich.
(79) Sharp, K. H., Mewies, M., Moody, P. C. E., and Raven, E. L. (2003) Crystal structure of the ascorbate peroxidase-ascorbate complex. *Nat. Struct. Biol. 10*, 303−307.

(80) Hornig, D. (1975) Distribution of ascorbic acid, metabolites and analogs in man and animals. *Ann. N.Y. Acad. Sci. 258*, 103−118.
(81) Martin, A., and Frei, B. (1997) Both intracellular and extracellular vitamin C inhibit atherogenic modification of LDL by human vascular endothelial cells. *Arterioscler. Thromb. Vasc. Biol. 17*, 1583−1590.